JACS
JOURNAL OF THE AMERICAN CHEMICAL SOCIETY
Article
pubs.acs.org/JACS

Structural Mechanism for the Fidelity Modulation of DNA Polymerase λ

Mu-Sen Liu,[†,§] Hsin-Yue Tsai,[†,∥] Xiao-Xia Liu,[†,#] Meng-Chiao Ho,[†,§] Wen-Jin Wu,*[,†] and Ming-Daw Tsai*[,†,‡,§]

[†]Institute of Biological Chemistry and [‡]Genomics Research Center, Academia Sinica, 128 Academia Road Sec. 2, Nankang, Taipei, 115, Taiwan

[§]Institute of Biochemical Sciences, National Taiwan University, Taipei 106, Taiwan

Supporting Information

ABSTRACT: The mechanism of DNA polymerase (pol) fidelity is of fundamental importance in chemistry and biology. While high-fidelity pols have been well studied, much less is known about how some pols achieve medium or low fidelity with functional importance. Here we examine how human DNA polymerase λ (Pol λ) achieves medium fidelity by determining 12 crystal structures and performing pre-steady-state kinetic analyses. We showed that apo-Pol λ exists in the closed conformation, unprecedentedly with a preformed MgdNTP binding pocket, and binds MgdNTP readily in the active conformation in the absence of DNA. Since prebinding of MgdNTP could lead to very low fidelity as shown previously, it is attenuated in Pol λ by a hydrophobic core including Leu431, Ile492, and the Tyr505/Phe506 motif. We then predicted and demonstrated that L431A mutation enhances MgdNTP prebinding and lowers the fidelity. We also hypothesized that the MgdNTP-prebinding ability could stabilize a mismatched ternary complex and destabilize a matched ternary complex, and provided evidence with structures in both forms. Our results demonstrate that, while high-fidelity pols follow a common paradigm, Pol λ has developed specific conformations and mechanisms for its medium fidelity. Structural comparison with other pols also suggests that different pols likely utilize different conformational changes and microscopic mechanisms to achieve their catalytic functions with varying fidelities.

INTRODUCTION

The structure and mechanism of DNA polymerases (pols) have been active subjects of research in the past six decades. The activities have intensified in recent years due to the discovery of low-fidelity and special-function pols in the past two decades.[1−6] While the pols responsible for DNA replication are required to perform catalysis with very high fidelity, those involved in DNA repair, translesion synthesis, and mutagenic functions often exhibit lower fidelity. Although earlier studies have focused on understanding how the high-fidelity pols achieve high fidelity,[7,8] recent interests have shifted to the reverse question: how the lower fidelity pols achieve low fidelity.[3,5,6,9−13] The paradigm in the mechanism of catalysis by high-fidelity pols includes two main features: DNA binding occurs before MgdNTP binding,[14,15] and then MgdNTP binding induces a functionally important conformational change from the open to the closed form.[16] However, it remains to be established whether this paradigm is applicable to low-fidelity pols.

The high-fidelity pols are mainly responsible for DNA replication and most of them belong to families A, B, and C. On the other hand, the lower-fidelity pols are often involved in maintaining the integrity of DNA, including DNA repair (X-family) and translesion synthesis (Y-family). Though the Y-family pols often show low fidelity toward normal DNA, they are usually designed to perform special functions with different mechanisms.[3] For example, Pol η adopts an open active site cleft, which enables it to faithfully bypass a stalked TT-dimer and allows subsequent DNA synthesis to continue by a replicative pol.[17−20] On the other hand, Pol ι uses a unique narrow active site to restrict the template 8-oxo-G to a *syn* conformation, and forms a correct 8-oxoG:dCTP Hoogsteen pair for an error-free bypass.[21] Other interesting examples include Rev1, which achieves its high specificity toward dG:dCTP incorporation by using protein groups to direct both the incoming dCTP and the template G evicted from DNA;[22] and Dpo4, which bypasses the 2-aminofluorene lesion via error-free and error-prone mechanisms, with the latter promoted by interactions between the enzyme and the bulky lesion.[23]

Our studies have focused on the X-family pols because they perform similar functions in base excision repair (BER) while covering a wide range of fidelity, allowing detailed examination

Received: December 22, 2015
Published: February 2, 2016

DOI: 10.1021/jacs.5b13368
J. Am. Chem. Soc. 2016, 138, 2389−2398

of the factors that govern the fidelity. Within the X-family pols, which include, among others, mammalian Pol β, Pol λ, Pol μ, terminal deoxynucleotidyl transferase (TdT),[24,25] and polymerase X from African swine fever virus (Pol X),[26] Pol β is at the high end of fidelity (1700−93000)[27] and Pol X at the low end (1.9−7700),[28] with Pol λ (30−9100, calculated from the reported error rates)[29] lying in-between. Pol β has been shown to follow a sequential ordered mechanism with binding of DNA preceding that of MgdNTP.[30,31] On the other hand, Pol X (consisting of only two of the four subdomains, palm and fingers) has been shown to bind MgdGTP tightly in the absence of DNA.[13] This was suggested as a mechanism to overcome Watson−Crick base pairing, leading to the very low fidelity of Pol X.[28]

The contrasting mechanisms between low- and high-fidelity pols in the X-family led us to ask how the medium-fidelity human Pol λ regulates its fidelity. The main function of Pol λ is DNA repair.[1,32,33] The full-length Pol λ is a 63.4 kDa pol possessing a nuclear localization signal segment (a.a. 1−35), a BRCT domain (a.a. 36−132), a serine-proline rich domain (a.a. 133−243), and a Pol β-like catalytic core domain (a.a. 244−575).[32] The latter (39 kDa) has been used in most structural and kinetic studies of Pol λ in previous reports and in this work. It has been shown that the structure of Pol λ:DNA binary complex is already closed and does not further undergo dNTP-induced conformational change during catalysis.[34,35] However, whether the conformation of apo-Pol λ is open or closed remains unknown, and the structural basis for its medium fidelity remains unclear.

The results of this study indicate that Pol λ can form binary complexes with MgdNTP specifically, with highest affinity for MgdATP, in the absence of DNA. In addition, we report 12 crystal structures of Pol λ in three new forms: apo-Pol λ, binary complexes with the four MgdNTPs, and a dG:dATP (*anti*:*syn*) mismatched ternary complex. The structures of apo-Pol λ and the four binary complexes all exist in a closed conformation similar to that of the Pol λ:DNA binary complex. Unprecedentedly, the MgdNTP binding pocket is already preformed in apo-Pol λ. On the basis of the structural information, we predicted and observed that L431A mutation facilitates MgdNTP prebinding. We then elucidated the structural basis for the enhanced prebinding ability of L431A, and showed, by pre-steady-state kinetics, that the fidelity of L431A is indeed lowered relative to that of wild type (WT) Pol λ.

MATERIALS AND METHODS

This section describes only a summary of key materials and experimental methods. Detailed experimental procedures are described in Supporting Information (SI) Materials and Methods.

Protein Expression and Purification. Human Pol λ (a.a. 242−575) subcloned in the pET-22b vector was expressed in BL21 (DE3) Codon plus RIPL *E. coli* cells grown in LB media. The protein was purified as previously described.[34] The mutants L431A, Y505F and Y505A were generated with the QuikChange kits (Stratagene).

Crystallization, Data Collection and Structural Determination. All purified Pol λ and mutants samples were concentrated to 15 mg/mL for crystallization. The crystals were grown using the hanging-drop vapor diffusion method. Details of crystallization, data collection, and structural determination are described in Supporting Information. All structural figures were prepared using PyMOL.[36] All structural superimpositions were performed with the align module under PyMOL. The cavity introduced in the L431A mutant shown in Figure 3B was analyzed using the cavity_cull module under PyMOL. The following published PDB entries of Y-family pols were used for structural analysis: 1T94[37] for apo-Pol κ, 2OH2[38] for ternary Pol κ, 2RDI[39] for apo-Dpo4, 1JX4[40] for ternary Dpo4, 1JIH[17] for apo-Pol η, and 3MFH[18] for ternary Pol η.

Isothermal Titration Calorimetry (ITC) Measurements. All ITC experiments were performed on an ITC200 calorimeter (MicroCal Inc.). The heat evolved following each titration point was obtained from the integral of the signal, and the data were analyzed by the Microcal Origin software.

Pre-Steady-State Kinetics. All kinetic parameters (k_{pol} and $K_{d,app}$) were measured from pre-steady-state kinetics with details described in SI. The fidelity is defined as $[(k_{pol}/K_{d,app})_{correct} + (k_{pol}/K_{d,app})_{incorrect}]/(k_{pol}/K_{d,app})_{incorrect}$.[41]

RESULTS

Pol λ Can Bind MgdNTPs Selectively in the Absence of DNA. We first determined the binding affinity of Pol λ for MgdNTP by ITC (Figure S1A−D). As shown in Table 1 (row 1), Pol λ can bind all four MgdNTPs with the highest affinity for MgdATP (K_d^{MgdNTP} = 3.3 ± 0.5 μM) and the lowest for MgdGTP (K_d^{MgdNTP} = 45 ± 2 μM). These data suggest that Pol λ can bind MgdNTP with specificity in the absence of DNA.

Table 1. K_d^{MgdNTP} Values for the Binding of dNTP to Apo-Pol λ Determined by ITC[a]

Pol λ	metal ion	dGTP (μM)	dATP (μM)	dCTP (μM)	dTTP (μM)
WT	Mg^{2+}	45 ± 2[b]	3.3 ± 0.5	15 ± 1	38 ± 2
L431A	Mg^{2+}	6.3 ± 0.5	0.7 ± 0.2	1.4 ± 0.3	6 ± 1
Y505A	Mg^{2+}	n.d.[c]	53 ± 9	84 ± 3	n.d.[c]
Y505F	Mg^{2+}	89 ± 2	9.6 ± 0.3	23.3 ± 0.8	77 ± 8

[a]All Pol λ samples contained 50 mM borate/NaOH, 150 mM KCl, 2 mM NaN_3, and 4 mM $MgCl_2$ at pH 6.5. [b]The ± values stand for standard deviation from three repeats. [c]n.d.: nondetectable (the binding is too weak and beyond the detection limit).

Apo-Pol λ Exists in the Closed Conformation with Preformed dNTP Binding Pocket. We solved a total of 12 crystal structures of apo-Pol λ and its binary and ternary complexes. Detailed data collection conditions and structural parameters are described in SI Materials and Methods and in Table S1. The structural forms, crystallization approaches, and the PDB ID codes are listed in Table 2. As also shown in the column 4 of Table 2, some of the structures consist of the whole 39 kDa protein construct while some other crystals are without the 8 kDa lyase subdomain due to cleavage in crystallization, which has also been shown to occur in several reports for Pol β.[42−44] For Pol β, the structure is largely unaffected by the presence or absence of the 8 kDa subdomain.[42] We showed the same for Pol λ by comparing the structures of both forms (with and without the 8 kDa subdomain), for both apo-Pol λ and Pol λ:MnMgdCTP binary complex as described later. Unless otherwise specified, all structures described in the main text contain the whole 39 kDa construct, while the truncated structures are shown in SI.

Figure 1A shows the structure of apo-Pol λ (structure 1a in Table 2). In contrast to Pol β,[42] both the 8 kDa subdomain (which closes upon binding of DNA in Pol β) and the N-helix (which closes upon binding of correct MgdNTP) are already closed in apo-Pol λ (Figure 1B). This closed structure of apo-Pol λ resembles the recently published structure of apo-Pol μ,[45] though there are distinct differences as addressed in the Discussion. The closed N-helix is also observed for the two

DOI: 10.1021/jacs.5b13368
J. Am. Chem. Soc. 2016, 138, 2389−2398

Table 2. Summary of Pol λ Structures and Relevant Information

complex form	structure no.	metal ion	8 kDa[a]	crystallization approach	YF[b]	PDB codes
Apo-Pol λ	1a		+	Co^{2+} soak	⊥	5CB1
Apo-Pol λ	1b		−	Co^{2+} soak	⊥	5CB1
Apo-Pol λ	2a		−	Native	⊥	5DDM
Pol λ:dCTP	3a	$Mn^{2+}Mg^{2+}$	+	Mn^{2+} soak	⊥	5DDY
Pol λ:dCTP	3b	$Mn^{2+}Mg^{2+}$	−	Mn^{2+} soak	⊥	5DDY
Pol λ:dATP	4a	Mg^{2+}	−	MgdATP soak	⊥	4XQ8
Pol λ:dTTP	5a	Mg^{2+}	−	MgdTTP soak	⊥	4XRH
Pol λ:dGTP	6a	Mg^{2+}	−	MgdGTP soak	⊥	5CA7
Pol λ:dG:dATP ternary	7	Ca^{2+}	+	CadATP soak	⊥	5DKW
Apo-L431A	8a		−	Native	⊥	5CP2
L431A:dCTP	9a	Mg^{2+}	−	MgdCTP soak	∥[c]	5CR0
L431A:dTTP	10a	Mg^{2+}	−	MgdTTP soak	∥[c]	5CJ7
L431A:dGTP	11a	Mg^{2+}	−	MgdGTP soak	⊥	5CHG
L431A:dG:dCTP ternary	12	$Ca^{2+}Ca^{2+}$	+	Native	∥	5CWR

[a]The +/− signs designate that the 8 kDa subdomain is retained/truncated, respectively, as explained in the text. [b]Conformation of the YF (Tyr505-Phe506) motif; symbols "⊥" and "∥" represent perpendicular and parallel orientations, respectively, for the YF motif. [c]Flexible, with the majority in the parallel configuration as explained in Figure S5.

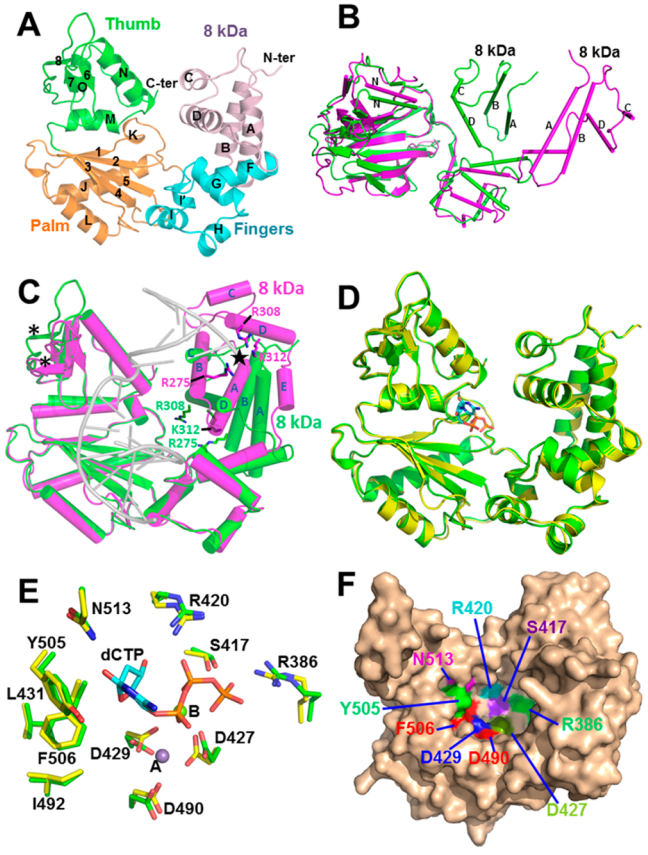

Figure 1. Comparison of apo-Pol λ with other relevant structures. (A) Structure of apo-Pol λ (structure 1a in Table 2). (B) Comparison between apo-Pol λ (green) and apo-Pol β (magenta, PDB code: 1BPD). (C) Overlay of apo-Pol λ (green) and Pol λ:DNA binary complex (protein in magenta, DNA in gray, 1XSN). Asterisk symbols indicate β-strand 8 location; black star indicates the location of downstream primer 5′-phosphate. (D) Overlay of apo-Pol λ (green) and Pol λ:MnMgdCTP binary complex (structure 3a, yellow, with dCTP shown in sticks). (E) Expansion of D with the dCTP binding residues shown. (F) Surface representation of apo-Pol λ with the dCTP binding residues shown in E colored and labeled.

additional structures of apo-Pol λ without the 8 kDa subdomain (structures 1b and 2a) (Figure S2).

Since the structure of apo-Pol λ was obtained for the first time, it allowed detailed comparison with that of Pol λ:DNA binary complex (PDB code: 1XSL) reported previously.[34,35] As shown in Figure 1C, both structures pre-exist in the closed form, though the conformations of the β-strand 8 containing loop differ. Interestingly, this loop harbors the critical Lys544 residue for stabilizing a scrunched DNA.[46] In addition, a closer examination of the two structures reveals a substantial conformational change in the 8 kDa subdomain upon DNA binding, which will be elaborated in the Discussion.

As shown in Figure 1D, the structure of the Pol λ:MnMgdCTP binary complex (structure 3a) also exists in the closed conformation and overlays well with the structure of apo-Pol λ. This structure also overlays very well with the same complex without the 8 kDa subdomain (structure 3b), and the other three Pol λ:MgdNTP binary complexes (structures 4a, 5a, and 6a) (Figure S3A). Figure 1E further shows that the active site residues are almost unchanged between the apo-form and the binary complex with MnMgdCTP. These results indicate that there is almost no conformational change upon MnMgdCTP binding, and that the apo-form is ready to accept the dNTP substrate as shown by the surface representation (Figure 1F).

The higher MgdATP affinity than MgdTTP and MgdCTP (Table 1) can be attributed to the more extensive pi:pi interaction between Tyr505 and dATP (Figure 2A). On the other hand, the lowest affinity of MgdGTP was puzzling at first. However, a close examination of the structures reveals that the potential H-bond between Asn513 and dGTP could be attenuated by the steric clash between the C_β protons of Asn513 and the NH_2 protons of dGTP (Figure 2B, left). This steric hindrance is absent in the binary complex with dATP (Figure 2B, right).

Bound dNTP and Its Binding Site in the Binary Complex Adopt Conformations Very Similar to the Ternary Complex. Since the structure of Pol λ:DNA:NaMgdCTP ternary complex is available,[47] it is chosen for comparison with the Pol λ:MnMgdCTP binary complex (Figure 2C). Importantly, most of the interactions in the ternary complex already exist in the binary complex: in addition

DOI: 10.1021/jacs.5b13368
J. Am. Chem. Soc. 2016, 138, 2389−2398

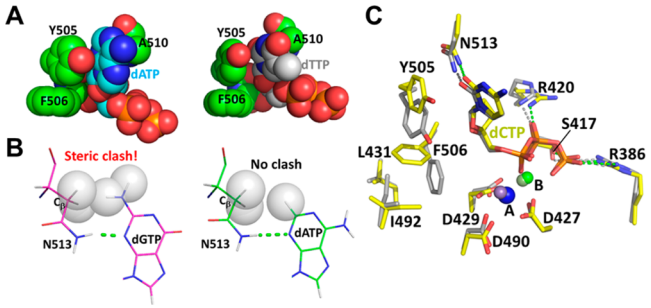

Figure 2. Structural basis for dNTP binding to Pol λ. (A) Structures showing more extensive pi:pi stacking between Tyr505 and dATP than dTTP (from structures 4a and 5a, respectively). (B) Structures showing potential steric clash between Asn513 C_β protons and dGTP NH_2 protons (left); no such steric clash is expected for dATP (right) (from structures 6a and 4a, respectively). The proton atoms were modeled using the h_add utility under PyMOL. (C) Overlay of the dNTP binding regions of the Pol λ:MnMgdCTP binary complex (yellow, structure 3a) and the Pol λ:DNA:NaMgdCTP ternary complex (gray, PDB code: 2PFP). Metal A is Na^+ (blue sphere) or Mn^{2+} (purple sphere) and metal B is Mg^{2+} (smudge sphere for the dCTP binary complex and green sphere for the ternary complex).

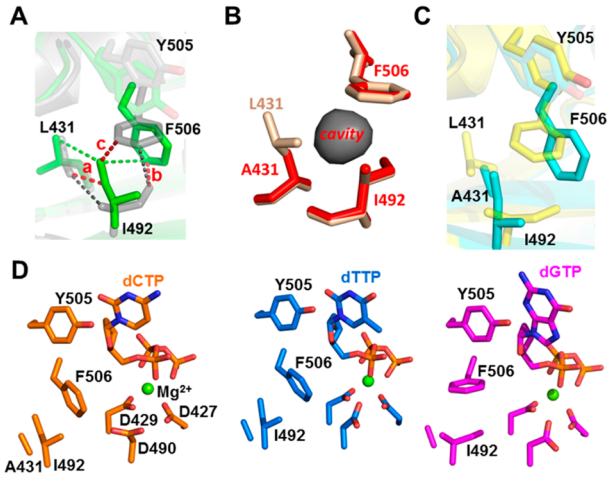

Figure 3. Conformations of the Tyr505/Phe506 motifs and bound dNTPs. (A) The structures of the YF motifs and surrounding regions for Pol λ:DNA (PDB code: 1XSL, gray) and Pol λ:DNA:MgdTTP (1XSN, green). (B) Overlay of apo-WT (structure 1a, wheat) and apo-L431A (structure 8a, red) showing the cavity introduced by the L431A mutation. (C) The structures of the YF motifs and surrounding regions for Pol λ:MnMgdCTP (structure 3a, yellow) and L431A:MgdCTP (structure 9a, cyan). (D) Structures of the YF motif regions in L431A:MgdNTP binary complexes (structures 9a, 10a, and 11a for dCTP, dTTP and dGTP, respectively).

to coordination between the three carboxylates and the two metal ions, γ-phosphate and β-phosphate of dCTP also form ionic interactions with side chains of Arg386 and Arg420, respectively, and Ser417 donates side chain O−H to form a potential H-bond with the γ-phosphate. In addition, remarkably, the bound nucleotides in the two complexes exist in almost the same conformation, ready for pairing with DNA even in the dNTP binary complex (Figure 2C). Furthermore, in the structures of the three Pol λ:MgdNTP binary complexes, the bound dNTPs also exist in this conformation (Figure S3B). Taken together with the preceding section, the results suggest that the MgdNTP binding pocket in the ternary complex is already in place in the apo-form. This preformed dNTP binding pocket in apo-Pol λ is unique and its potential functional significance will be further elaborated in Discussion.

The only notable difference between the two structures in Figure 2C is the orientations of the two aromatic rings of Tyr505 and Phe506 (the so-called YF motif[25]). In the Pol λ:DNA:NaMgdCTP ternary complex, the aromatic rings of Tyr505 and Phe506 are parallel to each other and form a partial pi:pi stacking interaction,[47] which has also been observed for the corresponding residues of Tyr271 and Phe272 in Pol β.[48,49] On the other hand, the YF motif has the two aromatic rings perpendicular to each other in the Pol λ:DNA binary complex.[35] In our structures of apo-Pol λ and Pol λ:MgdNTP binary complexes, the YF motifs all adopt perpendicular configurations (Table 2 and Figure 2C). Since parallel orientation of the YF motif has been suggested as an indication of the productive state of Pol λ previously,[50] our results suggest that even though MgdNTP and its direct binding residues exist in the active conformations, the protein part of the MgdNTP binary complexes is not yet in the catalytically active form.

Prediction and Demonstration that L431A Facilitates MgdNTP Binding in the Absence of DNA. Computational studies suggested that Ile492 may hinder the rotation of Phe506, thus regulate the conversion from the "pre-nucleotide binding state" (binary complex with DNA) to the "pre-catalytic state" (ternary complex).[50] Our further analysis indicates that the side chain conformation of Ile492 is in turn controlled by that of Leu431. Figure 3A overlays the side chains of Leu431, Ile492, Tyr505 and Phe506 in the Pol λ:DNA binary complex and the Pol λ:DNA:MgdTTP ternary complex. The comparison between these two forms shows that the transition from the binary to the ternary complexes involves rotation of the side chains of all three residues. The green and gray dashed lines indicate distances for hydrophobic interactions within each structure (3.8−4.2 Å), which all fall into the normal distances. Importantly, the red dashed lines with intercarbon distances of 2.5−2.6 Å indicate "steric clashes" between the two structures. On the basis of the red lines, Leu431 has to rotate before Ile492 does, otherwise it would create a clash (red line a). In addition, Ile492 and Phe506 have to rotate simultaneously since if only Phe506 rotates, there would be a clash (red line b); likewise, rotating Ile492 alone without rotating Phe506 would create another clash (red line c). In sum, our analysis suggests that Ile492 can regulate the conformational alteration of Phe506, and it is in turn regulated by the side chain flipping of Leu431.

On the basis of these analyses, we predicted that mutation of bulky Leu431 to the smaller Ala residue may facilitate the conformational rearrangement of the YF motif, which may in turn facilitate prebinding of MgdNTP in the absence of DNA. Indeed, the affinity of apo-L431A toward MgdNTP was enhanced by 7.2, 4.7, 10.5, and 6.3 folds for dGTP, dATP, dCTP and dTTP, respectively (Table 1 and Figure S1E-H).

The YF Motif Favors Parallel Orientation in the L431A:MgdCTP Binary Complex. We then solved the crystal structures of apo-L431A and three L431A:MgdNTP binary complexes (dCTP, dTTP and dGTP) (structures 8a, 9a, 10a, 11a, respectively). The overall structure of apo-L431A is very similar to that of apo-Pol λ, and the YF motif remains in the perpendicular orientation (Figure S4A). In addition, the global conformation of the three L431A:MgdNTP complexes overlay very well among themselves and also with that of the WT Pol λ:MnMgdCTP binary complex (Figure S4B), and the conformations of bound MgdNTP in the L431A:MgdNTP binary complexes (dCTP, dTTP and dGTP) are nearly

DOI: 10.1021/jacs.5b13368
J. Am. Chem. Soc. 2016, 138, 2389−2398

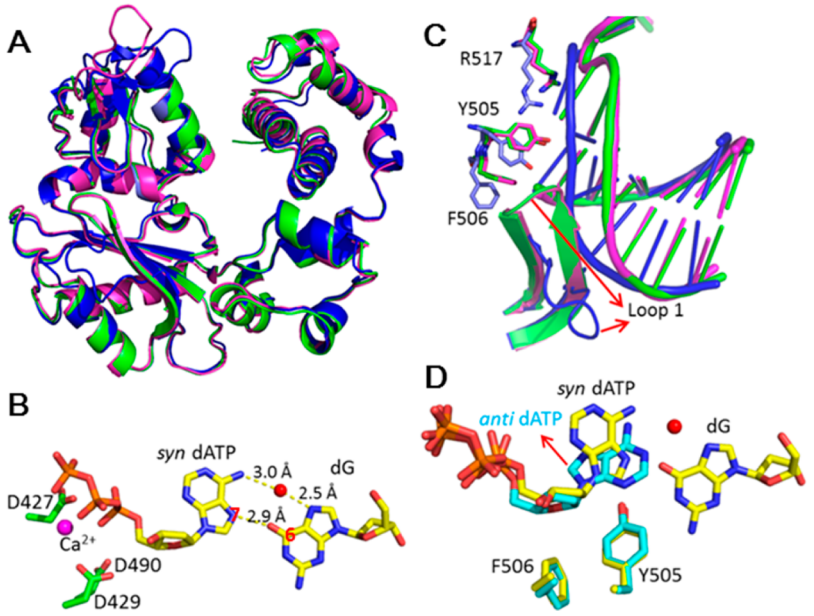

Figure 4. Structural information for the dG:CadATP mismatched ternary complex of WT Pol λ (structure 7). (A) Overlay of the structures (protein only) of the mismatched ternary complex of WT Pol λ with a dG:CadATP nascent base pair (green), the Pol λ:DNA binary complex (magenta, PDB code: 1XSL), and the dA:MgddTTP matched ternary complex (blue, PDB code:1XSN). (B) Nucleotide binding site structure of the mismatched ternary complex of Pol λ with dG:CadATP. (C) Overlay of the DNA site structures of the three complexes mentioned in A, with the same color codes. (D) Overlay of the nucleotide binding site structures of the dG:CadATP mismatched ternary complex of Pol λ with that of the Pol λ:MgdATP binary complex (structure 4a).

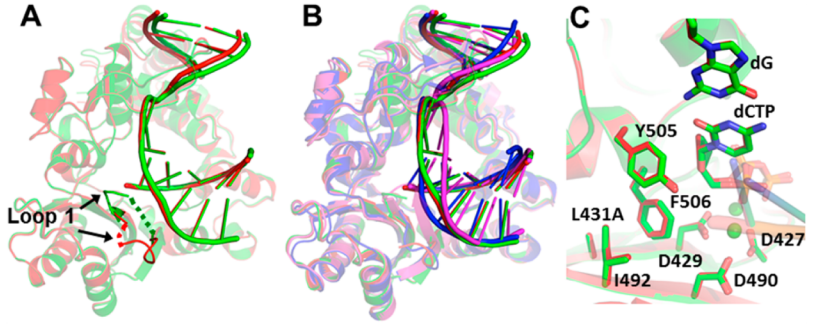

Figure 5. Two conformers in the crystal structure of the L431A:dG:CadCTP matched ternary complex (structure 12). (A) The two conformers A (red) and B (green) differ slightly in the conformations of loop 1 and the template DNA strand. The segments with missing electron densities in loop 1 (Gln469 in conformer A, Glu465-Asn467 in conformer B) are shown as dashed lines. (B) Overlay of the structures of conformer A (red), conformer B (green), WT Pol λ:DNA binary complex (magenta, PDB code: 1XSL), and WT Pol λ:DNA:MgdTTP ternary complex (blue, 1XSN). (C) Active site structures of the two conformers. Mg^{2+} ions are shown in green spheres.

unchanged from that in the WT Pol λ:MnMgdCTP binary complex (Figure S4C).

The results described above indicate that the L431A mutation did not affect the conformations of the MgdNTP binding residues and the bound dNTPs. Thus, the enhanced affinity of L431A (relative to WT) for MgdNTP can be attributed to the L431A mutation as predicted. The detailed molecular basis of this effect is further explained here. As shown in Figure 3B, structural comparison confirms that a cavity is created at the Ala431 site in the apo-L431A mutant. Figure 3C shows the active site geometry of the L431A:MgdCTP binary complex (structure 9a) in comparison with the corresponding WT binary complex (structure 3a). As expected, the cavity created by the L431A mutation provides space for Ile492 to move away from the Phe506 ring, and allows Phe506 to rotate to the predominantly parallel position relative to Tyr505 for dCTP and dTTP though not dGTP (Figure 3D). Understandably, the cavity also provides conformational flexibility for Phe506, leading to missing electron densities for the C_ε and C_ζ carbons of the aromatic ring (Figure S5A) and high B-factors (Figure S5B). Taken together, the results support that Leu431 is a key residue controlling the rotation of the YF motif in Pol λ.

High Affinity for MgdATP Facilitates Formation of a Mismatched Ternary Complex of Pol λ with dG:dATP. On the basis of the ability of Pol λ to bind MgdATP tightly, we speculated that there is a likelihood of solving the structure of a mismatched ternary complex involving MgdATP, and indeed succeeded in solving the mismatched ternary complex structure of WT Pol λ with a dG:dATP nascent base pair in the presence of Ca^{2+} ions (structure 7). As shown in Figure 4A, Pol λ of the mismatched ternary complex adopts a closed conformation similar to the Pol λ:DNA binary complex (PDB code: 1XSL) and the dA:ddTTP matched ternary complex (PDB code:

DOI: 10.1021/jacs.5b13368
J. Am. Chem. Soc. 2016, 138, 2389−2398

Table 3. Summary of Pre-Steady-State Kinetic Data

base pair	$K_{d,app}$ (μM)	k_{pol} (s^{-1})	mutant $k_{pol}/K_{d,app}$ ($\mu M^{-1} s^{-1}$)	mutant fidelity[a]	WT[b] $k_{pol}/K_{d,app}$ ($\mu M^{-1} s^{-1}$)	mutant ($k_{pol}/K_{d,app}$)/WT ($k_{pol}/K_{d,app}$)
dA:dATP	2.1 ± 0.4[c]	0.005 ± 0.0005	2.3×10^{-3}	1400	2.8×10^{-4}	8.2
dA:dGTP	6.2 ± 0.8	0.024 ± 0.002	3.9×10^{-3}	820	2.6×10^{-3}	1.5
dA:dCTP	0.42 ± 0.04	0.052 ± 0.001	1.3×10^{-1}	26	1.1×10^{-2}	11.8
dA:dTTP	3.3 ± 0.2	10.6 ± 0.1	3.2	1	2.5	1.3
dG:dATP	0.9 ± 0.1	0.0017 ± 0.0004	1.9×10^{-3}	1100	6.7×10^{-4}	2.8
dG:dCTP	1.4 ± 0.2	2.8 ± 0.2	2.1	1	2.7	0.78
dC:dATP	0.411 ± 0.002	0.0099 ± 0.0004	2.4×10^{-2}	65	3.2×10^{-3}	7.5
dC:dGTP	4.5 ± 1.2	6.5 ± 0.7	1.6	1	2.1	0.76
Y505A[d]						
dA:dGTP	30 ± 3	0.00075 ± 0.00002	2.5×10^{-5}	5.2×10^{4}	2.6×10^{-3}	0.01
dA:dTTP	1.0 ± 0.1	1.30 ± 0.03	1.3	1	2.5	0.52

[a]The fidelity is defined by $[(k_{pol}/K_{d,app})_{correct} + (k_{pol}/K_{d,app})_{incorrect}]/(k_{pol}/K_{d,app})_{incorrect}$. [b]WT data are taken from Fiala et al.[29] [c]The ± values stand for standard deviation from three repeats. [d]Y505A data are taken from Brown et al.[51]

1XSN). As shown in Figure 4B (with the electron density map shown in Figure S6), the dG:dATP mismatch assumes an *anti*:*syn* conformation, which is stabilized by a water molecule between the amino NH_2 group of dATP and N7 of dG. In addition, the distance between the N7 of dATP and O6 of dG is only 2.9 Å, suggesting a possible hydrogen bond. In that case, the guanine base of dG may adopt an enol form with a C6-OH group to act as an H-bond donor.

The detailed structure of the mismatched complex is more similar to that of the Pol λ:DNA binary complex than the matched dA:ddTTP ternary complex. As shown in Figure 4C, no substantial conformational changes were observed for the template DNA strand, the loop 1, and the protein side chains of Arg517, Tyr505 and Phe506 between the Pol λ:DNA binary complex (in magenta color) and the dG:dATP mismatched ternary complex (in green color). The orientation of the YF motif remains perpendicular, and the dATP in the mismatched ternary complex remains in the same conformation as in the Pol λ:MgdATP binary complex (structure 4a), except that the base of dATP is rotated from an *anti* conformation to a *syn* conformation so that the base is coplanar with the templating dG in order to form a hydrogen bond (Figure 4D).

L431A May Destabilize the Matched Ternary Complex. We also speculated that the cavity and flexibility of the active site of L431A as described above may destabilize the matched ternary complex. In support, we solved the crystal structure of the L431A:dG:CadCTP matched ternary complex (structure 12) and found that the crystal consists of two molecules with different conformations in each asymmetric unit (ASU) (Figure 5A), designated as conformer A and conformer B. As shown in Figure 5A, the two conformers differ in the conformations of loop 1 and also slightly in the template DNA strand. One of the unique structural characteristics of Pol λ is a shift of the DNA position between the binary complex and the ternary complex.[35] As shown in Figure 5B, the conformations of the template DNA for both conformers fall between those of WT Pol λ:DNA binary complex and WT matched ternary complex, even though the global conformations of the proteins are the same. In addition, as shown in Figure 5C, the active site structures of the two conformers are nearly identical and the YF motif turns to a parallel orientation in both complexes (the electron density maps are shown in Figure S7), similar to that of the matched ternary complexes of WT (Figure 2C).

L431A Lowers the Fidelity Based on Pre-Steady-State Kinetic Analysis. The above results taken together suggest that the fidelity of L431A should be lowered relative to WT, based on our previous report that prebinding of MgdNTP in the absence of DNA could facilitate non-Watson−Crick incorporation.[13] To provide further support for this possibility, we performed pre-steady-state kinetic analysis for L431A and the results are summarized in Table 3. To ensure that our L431A fidelity can be compared with the WT fidelity reported previously,[29] we used the same gapped DNA and identical conditions and showed that the $K_{d,app}$ and k_{pol} values of dG:dCTP incorporation catalyzed by our WT Pol λ are the same as the reported values within ±10%. We then determined the $K_{d,app}$ and k_{pol} values of L431A for dN:dATP and dA:dNTP incorporations since dATP is most preferred by L431A (Table 1). As shown by the data in Table 3 and Figure 6, the $k_{pol}/K_{d,app}$ values of L431A are within ±30% relative to WT for matched incorporations, but are generally higher (1.5 to 12 folds) for mismatched incorporations, indicating lowered fidelity for L431A.

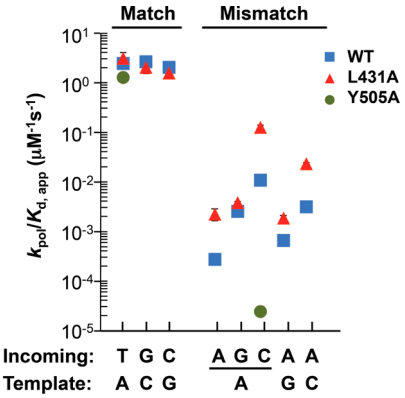

Figure 6. Plots of the $k_{pol}/K_{d,app}$ values of WT versus mutants as a summary of the data in Table 3.

Y505A Mutant Changes in the Opposite Way Relative to L431A. By examining the structures of the seven dNTP binary complexes described above, we found that a unique stabilizing force for the binary complex (relative to the ternary complexes) is the partial pi:pi ring stacking between Tyr505 and the nucleotide base (Figure 2A,B). This property of Tyr505 is similar to that of His115 in the Pol X:MgdGTP binary complex.[13] We reasoned that disrupting the ring stacking interaction in the binary complex should perturb the dNTP

DOI: 10.1021/jacs.5b13368
J. Am. Chem. Soc. 2016, 138, 2389−2398

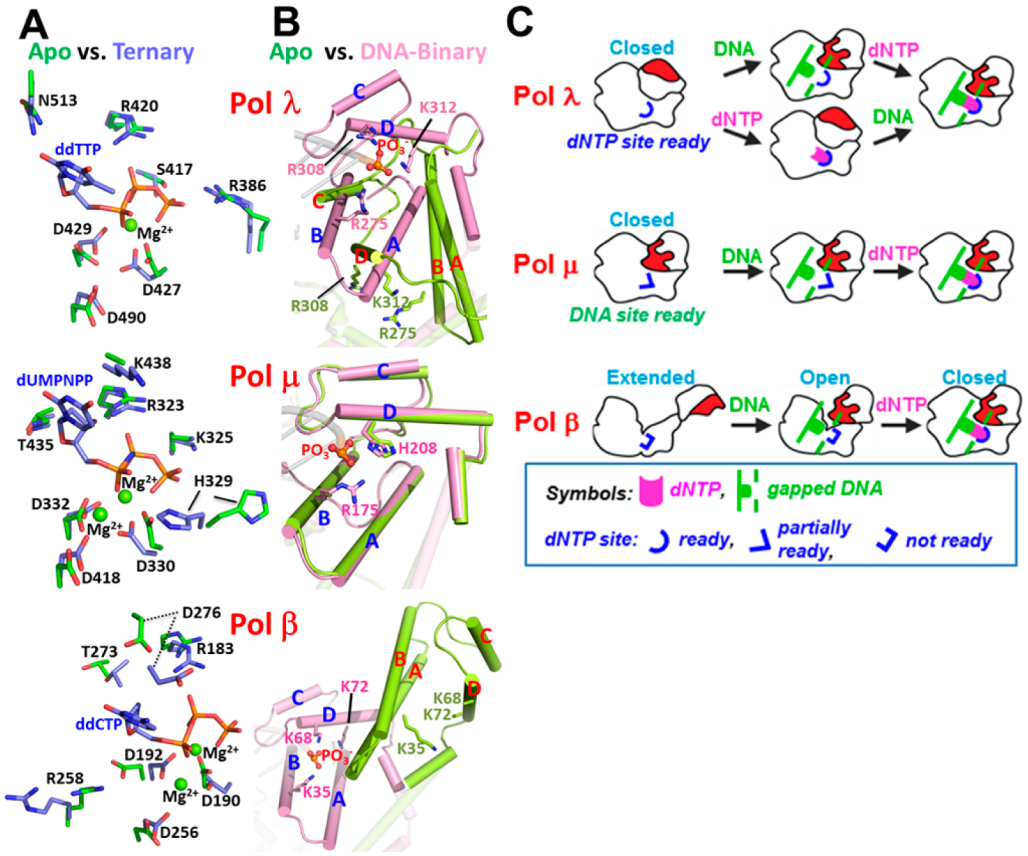

Figure 7. Apo-Pol λ preforms MgdNTP binding pocket while apo-Pol μ preforms DNA binding site. (A) Comparison between Pol λ, Pol μ, and Pol β on the MgdNTP binding pocket residues (apo-forms in green and pol:DNA:MgdNTP ternary complexes in slate). (B) Comparison between Pol λ, Pol μ, and Pol β on the conformational transition of the 8 kDa subdomain going from apo-form (lemon) to pol:DNA binary complexes (protein in pink, DNA in gray). PDB codes: apo-Pol λ (5CB1), apo-Pol β (1BPD), apo-Pol μ (4LZD), Pol λ:DNA Binary (1XSL), Pol β:DNA Binary (1BPX), Pol μ:DNA Binary (4LZG), Pol λ:DNA:MgddTTP Ternary (1XSN), Pol β:DNA:MgddCTP Ternary (1BPY), Pol μ:DNA:MgdUMPNPP Ternary (4M04). (C) Cartoon illustration for the structural comparisons in (A) and (B).

binding affinity in the absence of DNA. As shown in Table 1 (rows 3–4) and Figure S1I–N, we found that the binding of all four MgdNTPs was substantially weakened in the Y505A mutant, but only modestly affected in Y505F. Furthermore, the fidelity of Y505A is expected to be enhanced, which is supported by the fidelity data reported previously,[51] as also listed in Table 3 and Figure 6.

DISCUSSION

Major Advances and Significance. Two major advances have been achieved in this work. First, we showed that Pol λ likely achieves its medium fidelity by prebinding MgdNTP in the absence of DNA to lower the fidelity, and attenuating its prebinding ability by a hydrophobic cluster. The balance between these two mechanisms can explain why the fidelity of Pol λ is lower than that of Pol β (which cannot prebind MgdNTP) but higher than that of the Pol X (which can prebind MgdNTP more tightly overall). Disruption of the attenuation mechanism by the L431A mutation enhanced the binding affinity of Pol λ for MgdNTP and lowered its fidelity.

Second, we found that apo-Pol λ not only pre-exists in the closed form like Pol μ, but also preforms its MgdNTP binding pocket (which is not the case for Pol μ). Detailed comparison between Pol λ, Pol μ, and Pol β led to the interesting finding that the three representative human DNA repair pols differ in their structural mechanisms—the MgdNTP binding pocket is preformed in apo-Pol λ but not apo-Pol μ, the DNA binding site is preformed in apo-Pol μ but not apo-Pol λ, and neither occurs in apo-Pol β. These interesting comparisons are illustrated in Figure 7A,B and suggest that the structure and mechanism of each polymerase is likely optimized for its biological functions in the evolutional process.

Preformation of the MgdNTP Binding Pocket Is Unique to Apo-Pol λ. Our results show that the overall conformations of apo-Pol λ and its binary complexes with MgdNTPs are very similar to each other, and that MgdNTPs bind to the active site in a productive position, similar to that in the matched ternary complex. This property is different from that of Pol β and other high-fidelity replicative pols which cannot bind MgdNTP in the productive conformation in the absence of DNA. Although the crystal structure of the Pol β:dATP complex is available, dATP was shown to bind in an inactive conformation.[42] Nonproductive dNTP binding has also been reported for bacterial apo-Pol I,[52−54] and for TdT where the adenine N1 atom in the TdT:ddATP binary complex (PDB code: 1KEJ)[55] needs to shift ca. 6.2 Å to be superimposable with that in the TdT:ssDNA:dAMPcPP ternary complex (PDB code: 4I2E).[56] *Thermus thermophilus* HB8 Pol X has also been reported to prebind MgdNTP tightly, but it has little misincorporation activity.[57]

Since apo-Pol μ also exists in the closed conformation, we examined whether the MgdNTP binding pocket is also preformed in apo-Pol μ. The structural comparisons in Figure

DOI: 10.1021/jacs.5b13368
J. Am. Chem. Soc. 2016, 138, 2389−2398

7A show that, unlike Pol λ, the MgdNTP binding residues of Pol μ in the ternary complex are not fully in place in the apo-form (e.g., the His329 side chain). For reference, the same comparison for Pol β indicates that most MgdNTP binding residues are not in place in the apo form (e.g., Arg183, Asp192, Arg258 and Asp276). In summary, the MgdNTP binding pocket is preformed in apo-Pol λ, partially formed in apo-Pol μ, and not yet formed in apo-Pol β. Interestingly, even though the viral Pol X can prebind MgdGTP tightly, it undergoes a conformational change involving hydrophobic side chain rearrangements upon MgdGTP binding,[13] indicating that the MgdGTP binding pocket is not preformed in apo-Pol X. Thus, preformation of the dNTP binding pocket is unique to apo-Pol λ.

DNA Binding Site Is Preformed in Apo-Pol μ but Not Apo-Pol λ. Another interesting property of Pol λ is that even though both the apo-form and its binary complex with DNA exist in the closed conformation, the 8 kDa subdomain of Pol λ does undergo a notable conformational change upon DNA binding (Figure 1C, and Figure 7B for the expanded view) with Arg275, Arg308 and Lys312 moving 24 Å, 23 and 17 Å, respectively, in order to form tight electrostatic interactions with 5′-phosphate of the downstream primer. Again we examined this property in Pol μ for comparison, and found an interesting contrast—the DNA binding site of Pol μ is preformed in apo-Pol μ (Figure 7B).

Since Pol β also uses the 8 kDa subdomain to achieve its lyase function, the important question to ask is whether this DNA-induced conformational transition of the 8 kDa subdomain in Pol λ is similar to that of Pol β. The comparison reveals that the mode of conformational transition in Pol λ upon DNA binding is different from the large conformational change observed for Pol β (Figure 7B), although they achieve the same purpose of binding gapped DNA for BER and for lyase functions. The conformational transition of the 8 kDa subdomain in Pol λ appears to be a more complicated mode of rotational movements of several helices, while it is a much simpler mode of translational movement Pol β. We speculate that the simpler conformational change of the 8 kDa subdomain in Pol β than that of Pol λ may in part explain the much higher DNA affinity of Pol β (0.077 nM for a 36-mer gapped DNA)[58] than Pol λ (110 nM for a 41-mer gapped DNA),[51] which in turn may provide a structural basis for the primary role of Pol β in short-patch DNA BER and the backup role of Pol λ.[24,59−61]

Taken together, our results indicate that, even though both apo-forms of Pol λ and Pol μ exist in the "closed conformation", a property in contrast to high-fidelity pols, there are distinct differences in the properties of these two pols. To facilitate visualization, the structural comparisons in Figure 7A,B are summarized by cartoon illustrations in Figure 7C.

Comparison with Y-Family Polymerases. The structural basis of DNA binding of Y-family pols is substantially different from that of other families, as reviewed recently.[3] Since crystal structures of apo- and ternary forms are both available for Pol κ, Dpo4 and Pol η (PDB codes listed in Materials and Methods), we compared their MgdNTP binding pocket residues between these two forms, and found that the binding pocket is preformed in apo-Pol κ, partially formed in apo-Dpo4, but not ready in apo-Pol η, though a report indicated that the DNA-bound Pol η is prealigned to accept dNTP.[62] The results of such analyses suggest that, like the X-family pols, the MgdNTP binding pocket of Y-family pols is formed at different stages of catalysis, and is preformed in the apo-form for Pol κ. It will be interesting to elucidate whether and how these differences are related to their functions.

The Preformed MgdNTP Binding Pocket in Apo-Pol λ Could Facilitate Formation of the Mismatched dG:dATP Ternary Complex. In order to understand how a pol controls its fidelity, it is important to compare the structures of matched and mismatched ternary complexes. However, the latter is not favorable for crystallization, and crystal structures of a mismatched ternary complex with a nascent base pair are rare. For high-fidelity pols, it has been shown that the mismatched MgdNTP can only induce partial conformational closing based on SAXS analyses[44] and X-ray crystallography of Pol β[63,64] and the large fragment of *Bacillus* pol I.[65] A general approach to facilitate the formation and structural characterization of a mismatched ternary complex with a nascent base pairing is to introduce "mutagenic factors or mutations". On the basis of this concept, the mismatched ternary complex structures have been obtained for Pol β/Mn^{2+},[63,64] BF Pol/Mn^{2+},[12] a loop 1-deletion mutant of Pol λ,[66] and a L415A/L561A/S565G/Y567A quadruple mutant of RB69 (a B-family pol).[67] The only exception is the dG:MgdGTP ternary complex of WT Pol X[13] and the dG:CadATP ternary complex of WT Pol λ reported here, likely facilitated by the ability of these two pols to prebind MgdNTP in a productive conformation in the absence of DNA. Interestingly, these two mismatched base pairs both assume an *anti*:*syn* geometry, while all other mismatched complexes mentioned above adopt the *anti*:*anti* geometries similar to correct matches.

Pol λ Also Shows High Affinity for dNTP in the Presence of DNA. Pre-steady-state kinetic data suggest that the Pol λ:DNA binary complex has abnormally high affinity for incorrect dNTP[29,32] based on the comparable values of $K_{d,app}$ (or K_d in Fiala et al.[29]) between correct and incorrect dNTP, which is different from most pols for which the $K_{d,app}$ values are substantially higher for incorrect dNTP.[68] In addition, this property of Pol λ appears to be independent of the gap size of damaged DNAs.[69] Suo's group also performed site-directed mutagenesis to identify the residues involved in the tight binding of Pol λ:DNA binary complex for dNTP.[51]

In this work we address the dNTP affinity of Pol λ by a different approach and for a different purpose: to examine and compare the MgdNTP binding ability of apo-pols based on K_d^{MgdNTP} values, which differ from the property of $K_{d,app}$ in the catalytic condition. An evidence for the difference between these two properties is that the prebinding of Pol λ is highly specific to dATP (Table 1), while the $K_{d,app}$ value from pre-steady-state kinetics displayed little specificity toward different dNTPs.[29] The preference of Pol λ for dATP is also consistent with the previous report that Pol λ has a high tendency to incorporate a dATP across a 8-oxo-dG lesion, causing C:G to A:T transversion mutations.[70]

Potential Significance of the dNTP-Prebinding Ability in Catalysis and Biological Functions of Pol λ. Our results should not be taken to suggest that Pol λ cannot bind DNA before binding MgdNTP. The structure of the Pol λ:DNA binary complex has been well established as shown in Figure 1C, and the mismatch incorporation is still only a small fraction for Pol λ. Our results only suggest that the canonical pathway is likely not the exclusive one for Pol λ, as illustrated in Figure 7C. However, since the in vivo concentration of dNTP in a dividing cell is in the range of 5−50 μM[71] (comparable to the K_d^{MgdNTP} values in Table 1), while the concentration of damaged DNA is

DOI: 10.1021/jacs.5b13368
J. Am. Chem. Soc. 2016, 138, 2389−2398

presumably much lower, the dNTP prebinding mechanism of Pol λ should be possible in vivo.

Most importantly, our finding in the correlation between K_d^{MgdNTP} and fidelity may provide a molecular basis for the earlier reports that elevated and imbalanced level of dNTP increases the misincorporation or infidelity of pols.[72−75] In addition, Sweasy and co-workers showed that the colon cancer related mutant K289M displays higher mutation rate.[58] Furthermore, Albertella et al. showed that elevated level of Pol λ are found in various human tumor tissues (2.1−12.7 folds), while reduced level of Pol λ was also found in other type of tumor tissues.[76] The reduced level of this DNA repair enzyme in cancer is intuitively understandable since the unrepaired lesion could lead to cancer. On the other hand, the elevated level of Pol λ in tumors can be understood by our finding in this study: dNTP prebinding in the absence of DNA could compromise the subsequent base pairing and increase the chance of misincorporation.

■ ASSOCIATED CONTENT

Supporting Information

The Supporting Information is available free of charge on the ACS Publications website at DOI: 10.1021/jacs.5b13368.

SI Materials and Methods; Tables S1−S4; Figures S1−S6. (PDF)

■ AUTHOR INFORMATION

Corresponding Authors

*winston@gate.sinica.edu.tw

*mdtsai@gate.sinica.edu.tw

Present Addresses

‖Institute of Molecular Medicine, National Taiwan University, Taipei 100, Taiwan.

#Department of Biophysics, University of Texas Southwestern Medical Center, Dallas, Texas 75390, United States.

Notes

The authors declare no competing financial interest.

■ ACKNOWLEDGMENTS

This research was supported by funding from Ministry of Science and Technology (Grant No. MOST103-2113-M-001-016-MY3), Academia Sinica, and the Taiwan Protein Project (Grant No. MOST105-0210-01-12-01). We thank the National Synchrotron Radiation Research Center (NSRRC) for access to beamlines BL13B1, BL13C1 and BL15A1 (Hsin Chu, Taiwan), and SPring-8 for access to beamlines BL12B2 and BL44XU (Hyogo, Japan) under the proposal No. 2012A4015, 2012B4014, 2012B4005, 2013A4003, 2013B4008, and 2014A4013. We thank Drs. Kunkel, T. A. and Bebenek, K. for providing Pol λ constructs, Dr. Shu-Chuan Jao, Dr. Meng-Ru Ho and Szu-Huan Wang of the Biophysics Core Facility, Scientific Instrument Center at Academia Sinica for their assistance in ITC experiments, Drs. Kai-Fa Huang, Manuel Maestre-Reyna and Tzu-Ping Ko for the helpful discussion in the refinement statistics, Dr. Masato Yoshimura for the helpful discussion in the phase determination of the initial Pol λ:MgdCTP structure, Dr. Wei-Chao Lee for help in initial crystallization set up and helpful discussion, and Tong-You Wade Wei for helpful discussion.

■ REFERENCES

(1) Bebenek, K.; Pedersen, L. C.; Kunkel, T. A. *Biochemistry* **2014**, *53*, 2781.

(2) Beard, W. A.; Wilson, S. H. *Biochemistry* **2014**, *53*, 2768.

(3) Yang, W. *Biochemistry* **2014**, *53*, 2793.

(4) Maxwell, B. A.; Suo, Z. *Biochemistry* **2014**, *53*, 2804.

(5) Hübscher, U.; Maga, G. *Curr. Opin. Chem. Biol.* **2011**, *15*, 627.

(6) Goodman, M. F.; Woodgate, R. *Cold Spring Harbor Perspect. Biol.* **2013**, DOI: 10.1101/cshperspect.a010363..

(7) Xia, S.; Konigsberg, W. H. *Biochemistry* **2014**, *53*, 2752.

(8) Johnson, K. A. *Biochim. Biophys. Acta, Proteins Proteomics* **2010**, *1804*, 1041.

(9) Guilliam, T. A.; Jozwiakowski, S. K.; Ehlinger, A.; Barnes, R. P.; Rudd, S. G.; Bailey, L. J.; Skehel, J. M.; Eckert, K. A.; Chazin, W. J.; Doherty, A. J. *Nucleic Acids Res.* **2015**, *43*, 1056.

(10) Broyde, S.; Patel, D. J. *Nature* **2010**, *465*, 1023.

(11) Johnson, S. J.; Taylor, J. S.; Beese, L. S. *Proc. Natl. Acad. Sci. U. S. A.* **2003**, *100*, 3895.

(12) Wang, W.; Hellinga, H. W.; Beese, L. S. *Proc. Natl. Acad. Sci. U. S. A.* **2011**, *108*, 17644.

(13) Wu, W.-J.; Su, M.-I.; Wu, J.-L.; Kumar, S.; Lim, L.-h.; Wang, C.-W. E.; Nelissen, F. H. T.; Chen, M.-C. C.; Doreleijers, J. F.; Wijmenga, S. S.; Tsai, M.-D. *J. Am. Chem. Soc.* **2014**, *136*, 4927.

(14) McClure, W. R.; Jovin, T. M. *J. Biol. Chem.* **1975**, *250*, 4073.

(15) Fisher, P. A.; Korn, D. *Biochemistry* **1981**, *20*, 4560.

(16) Doublie, S.; Sawaya, M. R.; Ellenberger, T. *Structure* **1999**, *7*, R31.

(17) Trincao, J.; Johnson, R. E.; Escalante, C. R.; Prakash, S.; Prakash, L.; Aggarwal, A. K. *Mol. Cell* **2001**, *8*, 417.

(18) Silverstein, T. D.; Johnson, R. E.; Jain, R.; Prakash, L.; Prakash, S.; Aggarwal, A. K. *Nature* **2010**, *465*, 1039.

(19) Washington, M. T.; Prakash, L.; Prakash, S. *Cell* **2001**, *107*, 917.

(20) Nakamura, T.; Zhao, Y.; Yamagata, Y.; Hua, Y.-j.; Yang, W. *Nature* **2012**, *487*, 196.

(21) Kirouac, K. N.; Ling, H. *Proc. Natl. Acad. Sci. U. S. A.* **2011**, *108*, 3210.

(22) Nair, D. T.; Johnson, R. E.; Prakash, L.; Prakash, S.; Aggarwal, A. K. *Science* **2005**, *309*, 2219.

(23) Rechkoblit, O.; Kolbanovskiy, A.; Malinina, L.; Geacintov, N. E.; Broyde, S.; Patel, D. J. *Nat. Struct. Mol. Biol.* **2010**, *17*, 379.

(24) Yamtich, J.; Sweasy, J. B. *Biochim. Biophys. Acta, Proteins Proteomics* **2010**, *1804*, 1136.

(25) Moon, A. F.; Garcia-Diaz, M.; Batra, V. K.; Beard, W. A.; Bebenek, K.; Kunkel, T. A.; Wilson, S. H.; Pedersen, L. C. *DNA Repair* **2007**, *6*, 1709.

(26) Oliveros, M.; Yáñez, R. J.; Salas, M. a. L.; Salas, J.; Viñuela, E.; Blanco, L. *J. Biol. Chem.* **1997**, *272*, 30899.

(27) Ahn, J.; Kraynov, V. S.; Zhong, X.; Werneburg, B. G.; Tsai, M.-D. *Biochem. J.* **1998**, *331*, 79.

(28) Showalter, A. K.; Tsai, M.-D. *J. Am. Chem. Soc.* **2001**, *123*, 1776.

(29) Fiala, K. A.; Abdel-Gawad, W.; Suo, Z. *Biochemistry* **2004**, *43*, 6751.

(30) Tanabe, K.; Bohn, E. W.; Wilson, S. H. *Biochemistry* **1979**, *18*, 3401.

(31) Wang, T. S. F.; Korn, D. *Biochemistry* **1982**, *21*, 1597.

(32) García-Díaz, M.; Bebenek, K.; Sabariegos, R.; Domínguez, O.; Rodríguez, J.; Kirchhoff, T.; García-Palomero, E.; Picher, A. J.; Juárez, R.; Ruiz, J. F.; Kunkel, T. A.; Blanco, L. *J. Biol. Chem.* **2002**, *277*, 13184.

(33) van Loon, B.; Hübscher, U. *Proc. Natl. Acad. Sci. U. S. A.* **2009**, *106*, 18201.

(34) Garcia-Diaz, M.; Bebenek, K.; Krahn, J. M.; Blanco, L.; Kunkel, T. A.; Pedersen, L. C. *Mol. Cell* **2004**, *13*, 561.

(35) Garcia-Diaz, M.; Bebenek, K.; Krahn, J. M.; Kunkel, T. A.; Pedersen, L. C. *Nat. Struct. Mol. Biol.* **2005**, *12*, 97.

(36) *The PyMOL Molecular Graphics System*, Version 1.3r1; Schrödinger, LLC, 2010.

(37) Uljon, S. N.; Johnson, R. E.; Edwards, T. A.; Prakash, S.; Prakash, L.; Aggarwal, A. K. *Structure* **2004**, *12*, 1395.

DOI: 10.1021/jacs.5b13368
J. Am. Chem. Soc. 2016, 138, 2389−2398

(38) Lone, S.; Townson, S. A.; Uljon, S. N.; Johnson, R. E.; Brahma, A.; Nair, D. T.; Prakash, S.; Prakash, L.; Aggarwal, A. K. *Mol. Cell* **2007**, *25*, 601.
(39) Wong, J. H.; Fiala, K. A.; Suo, Z.; Ling, H. *J. Mol. Biol.* **2008**, *379*, 317.
(40) Ling, H.; Boudsocq, F.; Woodgate, R.; Yang, W. *Cell* **2001**, *107*, 91.
(41) Wong, I.; Patel, S. S.; Johnson, K. A. *Biochemistry* **1991**, *30*, 526.
(42) Sawaya, M. R.; Pelletier, H.; Kumar, A.; Wilson, S. H.; Kraut, J. *Science* **1994**, *264*, 1930.
(43) Pelletier, H.; Sawaya, M. R. *Biochemistry* **1996**, *35*, 12778.
(44) Tang, K.-H.; Niebuhr, M.; Tung, C.-S.; Chan, H.-c.; Chou, C.-C.; Tsai, M.-D. *Nucleic Acids Res.* **2008**, *36*, 2948.
(45) Moon, A. F.; Pryor, J. M.; Ramsden, D. A.; Kunkel, T. A.; Bebenek, K.; Pedersen, L. C. *Nat. Struct. Mol. Biol.* **2014**, *21*, 253.
(46) Garcia-Diaz, M.; Bebenek, K.; Krahn, J. M.; Pedersen, L. C.; Kunkel, T. A. *Cell* **2006**, *124*, 331.
(47) Garcia-Diaz, M.; Bebenek, K.; Krahn, J. M.; Pedersen, L. C.; Kunkel, T. A. *DNA Repair* **2007**, *6*, 1333.
(48) Kraynov, V. S.; Werneburg, B. G.; Zhong, X.; Lee, H.; Ahn, J.; Tsai, M. D. *Biochem. J.* **1997**, *323*, 103.
(49) Cavanaugh, N. A.; Beard, W. A.; Batra, V. K.; Perera, L.; Pedersen, L. G.; Wilson, S. H. *J. Biol. Chem.* **2011**, *286*, 31650.
(50) Foley, M. C.; Arora, K.; Schlick, T. *Biophys. J.* **2006**, *91*, 3182.
(51) Brown, J. A.; Pack, L. R.; Sherrer, S. M.; Kshetry, A. K.; Newmister, S. A.; Fowler, J. D.; Taylor, J.-S.; Suo, Z. *J. Mol. Biol.* **2010**, *403*, 505.
(52) Li, Y.; Kong, Y.; Korolev, S.; Waksman, G. *Protein Sci.* **1998**, *7*, 1116.
(53) Ollis, D. L.; Brick, P.; Hamlin, R.; Xuong, N. G.; Steitz, T. A. *Nature* **1985**, *313*, 762.
(54) Beese, L. S.; Friedman, J. M.; Steitz, T. A. *Biochemistry* **1993**, *32*, 14095.
(55) Delarue, M.; Boulé, J. B.; Lescar, J.; Expert-Bezançon, N.; Jourdan, N.; Sukumar, N.; Rougeon, F.; Papanicolaou, C. *EMBO J.* **2002**, *21*, 427.
(56) Gouge, J.; Rosario, S.; Romain, F.; Beguin, P.; Delarue, M. *J. Mol. Biol.* **2013**, *425*, 4334.
(57) Nakane, S.; Ishikawa, H.; Nakagawa, N.; Kuramitsu, S.; Masui, R. *J. Mol. Biol.* **2012**, *417*, 179.
(58) Lang, T.; Maitra, M.; Starcevic, D.; Li, S.-X.; Sweasy, J. B. *Proc. Natl. Acad. Sci. U. S. A.* **2004**, *101*, 6074.
(59) Braithwaite, E. K. *J. Biol. Chem.* **2005**, *280*, 18469.
(60) Beard, W. A.; Wilson, S. H. *Chem. Rev.* **2006**, *106*, 361.
(61) Wiederhold, L.; Leppard, J. B.; Kedar, P.; Karimi-Busheri, F.; Rasouli-Nia, A.; Weinfeld, M.; Tomkinson, A. E.; Izumi, T.; Prasad, R.; Wilson, S. H.; Mitra, S.; Hazra, T. K. *Mol. Cell* **2004**, *15*, 209.
(62) Ummat, A.; Silverstein, T. D.; Jain, R.; Buku, A.; Johnson, R. E.; Prakash, L.; Prakash, S.; Aggarwal, A. K. *J. Mol. Biol.* **2012**, *415*, 627.
(63) Freudenthal, B. D.; Beard, W. A.; Shock, D. D.; Wilson, S. H. *Cell* **2013**, *154*, 157.
(64) Koag, M.-C.; Lee, S. *J. Am. Chem. Soc.* **2014**, *136*, 5709.
(65) Wu, E. Y.; Beese, L. S. *J. Biol. Chem.* **2011**, *286*, 19758.
(66) Bebenek, K.; Pedersen, L. C.; Kunkel, T. A. *Proc. Natl. Acad. Sci. U. S. A.* **2011**, *108*, 1862.
(67) Xia, S.; Wang, J.; Konigsberg, W. H. *J. Am. Chem. Soc.* **2013**, *135*, 193.
(68) Roettger, M. P.; Fiala, K. A.; Sompalli, S.; Dong, Y.; Suo, Z. *Biochemistry* **2004**, *43*, 13827.
(69) Brown, J. A.; Pack, L. R.; Sanman, L. E.; Suo, Z. *DNA Repair* **2011**, *10*, 24.
(70) Maga, G.; Villani, G.; Crespan, E.; Wimmer, U.; Ferrari, E.; Bertocci, B.; Hubscher, U. *Nature* **2007**, *447*, 606.
(71) Traut, T. W. *Mol. Cell. Biochem.* **1994**, *140*, 1.
(72) Buckland, R. J.; Watt, D. L.; Chittoor, B.; Nilsson, A. K.; Kunkel, T. A.; Chabes, A. *PLoS Genet.* **2014**, *10*, e1004846.
(73) Bebenek, K.; Roberts, J. D.; Kunkel, T. A. *J. Biol. Chem.* **1992**, *267*, 3589.
(74) Kumar, D.; Abdulovic, A. L.; Viberg, J.; Nilsson, A. K.; Kunkel, T. A.; Chabes, A. *Nucleic Acids Res.* **2011**, *39*, 1360.
(75) Reichard, P. *Annu. Rev. Biochem.* **1988**, *57*, 349.
(76) Albertella, M. R.; Lau, A.; O'Connor, M. J. *DNA Repair* **2005**, *4*, 583.

DOI: 10.1021/jacs.5b13368
J. Am. Chem. Soc. 2016, 138, 2389−2398